

## DESIGN, PREPARATION, AND *IN SILICO* STUDY OF NOVEL CURCUMIN-BIPHENYL CARBONITRILE CONJUGATE AS NOVEL ANTICANCER DRUG MOLECULES

GEETA KRISHNAMURTHY , LAIRIKYENBAM DEEPTI ROY , JYOTSNA KUMAR\* , N MANIKANDA PRABU,  
POOJA GOUR , SHIVANJALI ESTHER ARLAND 

Department of Chemistry, FMPS, M. S. Ramaiah University of Applied Sciences, Bangalore, India.

\*Corresponding author: Jyotsna Kumar; \*Email: drkumarchem111@gmail.com

Received: 12 Jul 2022, Revised and Accepted: 13 May 2023

### ABSTRACT

**Objective:** To design and synthesize the novel curcumin derivatives of curcumin-biphenyl carbonitrile conjugate to study their ADMET, drug-like behaviour and cytotoxicity on PANC1 cell lines.

**Methods:** Binding affinity of designed novel Curcumin analogues were assessed by molecular docking against the target protein (KRAS). Structures of lately synthesized compounds were characterized by spectral analysis. ADMET (absorption, distribution, metabolism, excretion, and toxicity) drug-likenesses behaviour prediction of synthesized curcumin analogues was done by computational analysis. The stability of the synthesized curcumin analogues was carried out by force degradation method as per ICH guidelines. *In vitro* cytotoxic assessment of these novel compounds on PANC 1 cancer cell lines was assessed by MTT assay.

**Results:** Three hit molecules were identified, which had the best binding affinity against the target protein KRAS having a docking score of -7.21 for CD2, -7.05 for CD3, and -6.80 for CD1. Most of the Pharmacokinetic (ADME) parameters are found to be quite agreeable and in the satisfactory range. 1H-NMR, FTIR and Mass spectrographic methods confirmed the structures. All three synthesized novel curcumin analogues were stable for a period of three months. Results of anti-proliferative activities indicated their cogent anticancer activity against PANC 1 cell line (IC<sub>50</sub> = 67.51 μM @CD1, 45.27 μM @CD2 and 168.60 μg/ml @CD3).

**Conclusion:** This study demonstrated that curcumin-biphenylcarbonitrile conjugate could be used as a plausible pharmacophore for targeting KRAS protein and will be supportive to explore the new series of cogent curcumin derivatives as anticancer agents.

**Keywords:** Curcumin, Biphenyl-carbonitrile, KRAS protein, MTT, PANC1

© 2023 The Authors. Published by Innovare Academic Sciences Pvt Ltd. This is an open access article under the CC BY license (<https://creativecommons.org/licenses/by/4.0/>)  
DOI: <https://dx.doi.org/10.22159/ijap.2023v15i4.45811>. Journal homepage: <https://innovareacademics.in/journals/index.php/ijap>

### INTRODUCTION

Treating cancer is still one of the utmost medical challenges, though a lot of technical advancements are there in the same field. After the heart diseases, cancer is considered as a second major deadly disease with leading mortality rate [1, 2]. As per WHO (World Health Organization), it counts 9.6 million deaths in 2018 and over the period of next 20 y the number of affected persons is roughly anticipated to surge by 70%.

In 2020 due to Coronavirus disease-19 pandemic the, diagnostic work was hampered, and the death rate increased. The statistical data tells us that Pancreatic cancer is the fourth most common cancer, which causes the maximum deaths in 2021 [3].

Cancer arises mainly due to the loss of regulatory mechanisms of normal cells. Any alterations in the microenvironment of the cell lead to impairment and become the cause of continuous multiplication of cells forming a tumor [4, 5]. Many therapies for different cancers are being used, which mainly intercede with different signaling pathways [6, 7]. Researchers have documented several oncogenes which are quite active due to genetic modifications in different forms, such as amplification, mutations, rearrangement. Among this mounting list of oncogenes, KRAS (Kirsten at Sarcoma Virus) protein, a member of the RAS family, other two being NRAS and HRAS, signifies the most ubiquitous oncogene in human cancers. Many researchers reported that in PDAC (pancreatic ductal adenocarcinoma) RAS-mutant is mostly seen to about a frequency of 100% KRAS mutation [8, 9].

Till today the most practised treatments such as chemotherapy, radiation therapy, hormone therapy, immunotherapy, targeted therapy or even stem cell transplant etc. are associated with serious side effects. Hence, to overcome the issue of painful side effects, researchers started searching for other safe alternatives with less or no side effects and this aroused the interest of researchers in natural components.

Curcumin, a natural polyphenolic component in the form of golden pigment in turmeric is a component of cosmetics and nutrition supplements. It has kindled the interest of researchers due to its wide therapeutic properties such as antioxidant, anti-inflammatory, antimicrobial, antitumor etc. [10, 11]. *In vitro* and *in vivo* studies have confirmed that curcumin has anticancer properties and can be used to treat several types of cancer, including pancreatic cancer by modulating molecular targets and multiple cell signaling pathways [12].

In preclinical studies, curcumin derivatives were reported to have the ability to target the G-quadruplex of KRAS by forming a c-myc promoter sequence [13]. In recent years drug discovery is more focused on molecules comprising heterocyclic moiety due to their biological similarities and as they own extensive pharmacological properties [14-18].

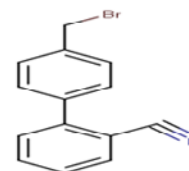


Fig. 1: Structure of 4'-(bromomethyl)-[1,1'-biphenyl]-2-carbonitrile

Among the heterocyclic compounds, aromatic carbo-nitrile are considered as very vital heterocyclic compounds with noteworthy pharmacological activities [19-23]. Biphenyl, with versatile efficacies and indispensable pharmacological activity, is a neutral molecule due to the absence of any active functional moiety. Therefore,

biphenyls with an active group can be further exploited for the synthesis of another active molecule of altogether new pharmacological activity.

Structurally Biphenyls are two abutted benzene rings which are attached through 1, 10-positions (fig. 1) [24]. The biaryl axis of biphenyl act as a central building block [25].

Another important pharmacophore, Nitrile group (-CN) is present in numerous anticancer agents, including letrozole to treat breast cancer [26], pelitinib and neratinib as EGFR (Estimated Glomerular Filtration Rate) inhibitors [27, 28], and bicalutamide a nonsteroidal androgen receptor antagonist to treat advanced prostate cancer [29–33].

Pervasive literature review suggested that scanty papers are reporting the anti-proliferative activity of synthesised curcumin derivatives conjugated with aromatic carbonitrile to impede the tumors. Ample biological and therapeutic values of aromatic nitrile compounds and curcumin incited us to develop novel curcumin analogues containing aromatic nitrile with good inhibitory activities.

In extension to our pursuit for novel natural heterocyclic-based anticancer agent, we choose for scaffold combination approach of drug design using curcumin as a scaffold comprising aromatic carbonitriles to synthesize curcumin-biphenylcarbonitrile conjugates (fig. 2).

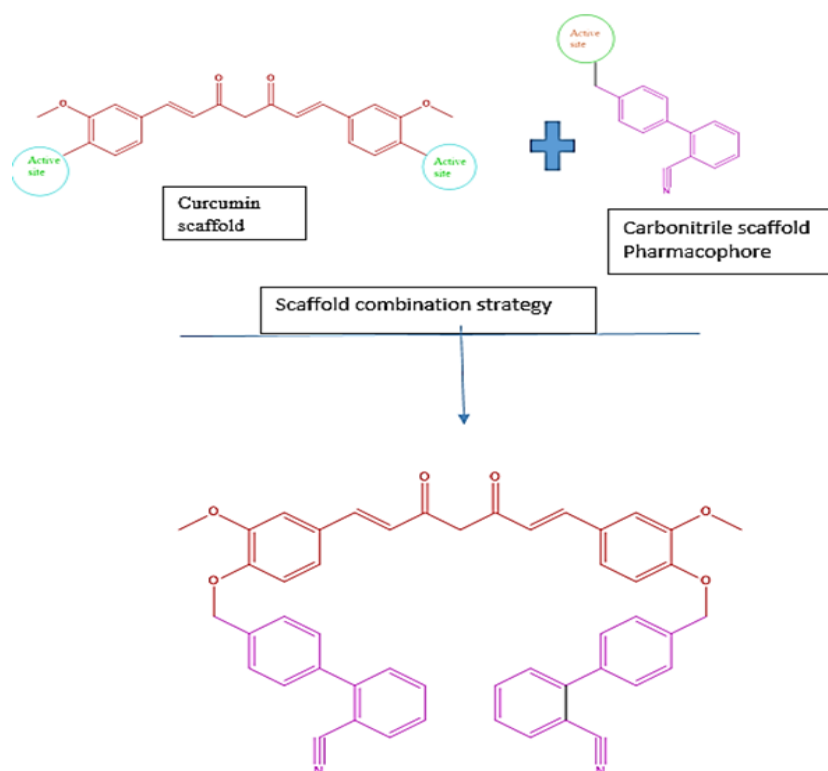


Fig. 2: Designed curcumin-biphenyl carbonitrile conjugate

Virtual screening of the designed curcumin derivatives was done to find their binding ability with the target protein KRAS (PDB code: 4EPV). Structures of synthesized hit molecules were confirmed by NMR (Nuclear Magnetic Resonance), FTIR (Fourier-transform Infrared) and Mass Spectroscopic methods. ADMET (Absorption, Distribution, Metabolism, Excretion, and Toxicity) profile of the selected derivatives was studied for their drug-likeness property. *In vitro* anticancer activity of these synthesized novel curcumin derivatives was carried on PANC1 (cancer cell lines).

## MATERIALS AND METHODS

### Materials

Analytical grade chemicals of 98% purity were purchased from Sigma Aldrich and used without further purification. For the characterization, NMR analysis was carried out by using a Bruker AV-III-400 MHz NMR spectrometer. LC-MS (Liquid chromatography-mass spectrometry) and IR (Infrared) spectroscopy were done on the LC-40 HPLC System (High-performance liquid chromatography, Shimadzu) and the Nicolet iS20 FTIR Spectrometer (Thermo Fisher Scientific™) respectively. The UV-2600 (UV-VIS Spectrophotometer from Shimadzu) was used to test the stability of the synthesized curcumin analogues. PANC1 (Pancreas) cell lines were obtained from the National Centre for Cell Line, Pune. DMEM (Dulbecco's Modified Eagle Media) with low

glucose-Cat No-11965-092 (Gibco, Invitrogen) FBS (Fetal bovine serum)-Cat No-10270106 (Gibco, Invitrogen). Anticancer potential was evaluated using ThermoFisher Scientific-Cat No. 15240062. Drug likeness and molecular properties of novel curcumin analogues were predicted using Molinspiration software, Swiss ADME, ADMET lab, and Syntelly software.

## Methodology

### Computational methodology

#### Ligand preparation

By adopting the scaffold combination approach, novel curcumin analogues were designed, where curcumin as a motif was functionalized with an aromatic carbonitrile moiety. Nine such curcumin analogues were designed and sketched using a 2D sketcher of the Maestro tool in Schrodinger software (table 1). To check the ionization conditions at neutral pH, 2D structures were preprocessed and then converted into ligands (3D structures) using the Lig-Prep tool of the Schrodinger software. The addition of hydrogen atoms, neutralization of charged groups, and optimization of the geometry of ligands were done using another tool called Epik [34, 35].

#### Protein selection, preparation, and validation

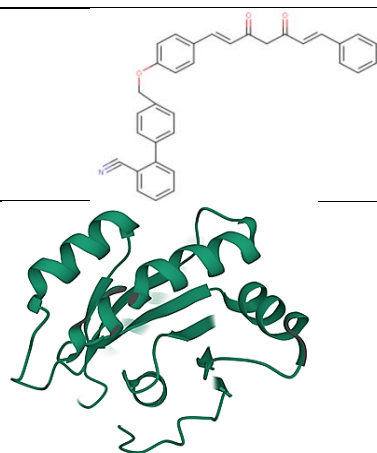
The KRAS protein (PDB code: 4EPV) was selected from the protein data bank and imported to the workplace (fig. 3). To obtain a clear

image, a protein from Homo sapiens with a resolution of 1.35 Å was chosen [36, 37].

**Table 1: Structures of newly designed curcumin derivatives (CD)**

S. No.	Structure	IUPAC name
CD1		4'-({4-[(1E,6E)-7-[4-({2'-cyano-[1,1'-biphenyl]-4-yl)methoxy}-3-methoxyphenyl]-3,5-dioxohepta-1,6-dien-1-yl]-2-methoxyphenoxy)methyl}-[1,1'-biphenyl]-2-carbonitrile
CD2		4'-({4-[(1E,6E)-7-[4-({2'-cyano-[1,1'-biphenyl]-4-yl)methoxy}phenyl]-3,5-dioxohepta-1,6-dien-1-yl]-2-methoxyphenoxy)methyl}-[1,1'-biphenyl]-2-carbonitrile
CD3		4'-({4-[(1E,6E)-7-[4-({2'-cyano-[1,1'-biphenyl]-4-yl)methoxy}phenyl]-3,5-dioxohepta-1,6-dien-1-yl]phenoxy)methyl}-[1,1'-biphenyl]-2-carbonitrile
CD4		4'-({4-[(1E,6E)-7-[4-({2'-cyano-4'-methyl-[1,1'-biphenyl]-4-yl)methoxy}-3-methoxyphenyl]-3,5-dioxohepta-1,6-dien-1-yl]-2-methoxyphenoxy)methyl}-4-methyl-[1,1'-biphenyl]-2-carbonitrile
CD5		4'-({4-[(1E,6E)-7-[4-({2'-cyano-4'-methyl-[1,1'-biphenyl]-4-yl)methoxy}phenyl]-3,5-dioxohepta-1,6-dien-1-yl]-2-methoxyphenoxy)methyl}-4-methyl-[1,1'-biphenyl]-2-carbonitrile
CD6		4'-({4-[(1E,6E)-7-[4-({2'-cyano-4'-methyl-[1,1'-biphenyl]-4-yl)methoxy}phenyl]-3,5-dioxohepta-1,6-dien-1-yl]phenoxy)methyl}-4-methyl-[1,1'-biphenyl]-2-carbonitrile
CD7		4'-({4-[(1E,6E)-7-[4-(4-hydroxy-3-methoxyphenyl)-3,5-dioxohepta-1,6-dien-1-yl]-2-methoxyphenoxy)methyl}-[1,1'-biphenyl]-2-carbonitrile
CD8		4'-({4-[(1E,6E)-3,5-dioxo-7-phenylhepta-1,6-dien-1-yl]-2-methoxyphenoxy)methyl}-[1,1'-biphenyl]-2-carbonitrile

CD9


COc1ccc(cc1)/C=C/C(=O)CC(=O)/C=C/c2ccccc2

**Fig. 3: X-Ray crystallographic structure of protein 4EPV**

The target protein GTPase KRAS has a sequence length of 170 amino acids that includes both polar and non-polar amino acids. The selected protein was prepared for docking using the Schrodinger suite's 'Protein preparation wizard' workflow [38].

The Lig-prep module of the Schrodinger suite was used to prepare the preprocessed ligand for docking. The SP mode via Glide of the Maestro tool of the Schrodinger suite was employed to dock it with the target protein. The target was superimposed on the preprocessed ligand and computed. The calculated root-mean-square deviation (RMSD) value was found to be 1.290 Å. The Superimposing of the docked ligand on the pre-processed ligand validates that the designed molecules can be docked with the target [39-41].

#### Receptor grid generation

Generation of the grid was done by using the Receptor Grid Generation tool of Schrodinger Software 2016 to identify the binding pocket where the molecule would bind with the target [42].

#### Glide ligand docking

Prepared Ligands and proteins were docked with standard precision using the Glide (grid-based ligand docking with energetics) algorithm in the Standard Precision (SP) mode. An Optimized Potentials for Liquid Simulations (OPLS) force field was used for all the calculations. All the Glide docking runs were performed on a Linux system. To compare the docking results of novel designed curcumin analogues, the docking of Gemcitabine, Dabrafenib, and curcuminoids were carried out with the same target [43-45].

#### ADMET studies

The pursuit of great target potency should not be pursued recklessly without an understanding of its significance towards effectiveness and efficiency. *In vitro* studies alone are not sufficient to judge the efficacy of synthesized drug candidates and their aptness as imminent drugs. Clinical trials of drug candidates with insufficient ADMET studies can cause irrevocable harm to biological systems. Therefore, studies for ADMET and drug-likeness behavior have become very critical steps in the journey of drug discovery, and of late, they have gained prominence. Hence, to save quality time and to get better results, prior to the synthesis of identified drug molecules, several pharmacokinetics parameters, such as absorption, distribution, metabolism, excretion, and toxicity, were calculated. The ADMET study comprises the absorption,

bioavailability, lipophilicity, quantitative measurement of drug-like properties, solubility, cell permeability, BBB (blood-brain-barrier) penetration, hepatic clearance, plasma-protein binding, metabolism, half-life, etc. [46, 47]. To study xenobiotic metabolism, a plethora of enzymes and proteins are involved, along with CYP450 enzymes.

Drug-likeness, ADMET, and toxicity profiles were analyzed using an online version of the Swiss ADME web tool, AdmetLab 2.0, and Syntelly. To execute this from the PubChem database, the Simplified Molecular Input Line Entry System (SMILES) layouts of all the ligands were obtained. To check the safety profile and oral activeness (drug-likeness) of all drug molecules in the human body, Lipinski's rule of 5 (a thumb rule developed by Christopher A. Lipinski in 1997) was applied towards all drug molecules. If the drug data corresponds to the given cut-off values, there is no violation of the Lipinski rule; if two or more violations are observed, the identified molecule's drug likeness is less [47]. By evaluating the standards allied with the immortalized human colorectal adenocarcinoma cell line (Caco-2), it is evident that Caco-2 cells are the best model to assess the cell permeability and the absorption of drug molecules (ligands) along with permeability (P)-glycoprotein inhibitor/substrate.

BBB and CNS (central nervous system) activity are equally important to be considered when the drug is acting peripherally in the range of 3 to 12.

To check the potential of a drug molecule to inhibit a particular cytochrome, cytochrome P450 (CYP450) isoforms enzymes (CYP1A2, CYP2C19, CYP2C9, CYP2D6, and CYP3A4) are important as these interactions may affect the plasma levels and potentially lead to toxicity. Most drugs that CYP450 also metabolize distress and hydroxylate various xenobiotics and endogenous compounds such as cholesterol, steroids, lipids, bile salts, or vitamins. Drug toxicity was studied mainly by considering AMES toxicity, human ether-a-go-go-related gene (hERG) inhibition, and hepatotoxicity.

All the significant ADMET parameters of all synthesized drug molecules were estimated and checked near to their amenability with respective standard ranges to identify their suitability as ideal drug candidates. These studies were performed by using the AdmetLab 2.0, Qikprop, Syntelly and SWISS ADME [46-48].

#### Synthesis

The synthesis of the hit-identified molecules was carried out in two steps: Step 1 consisting the separation of curcuminoids from turmeric to be used as a curcumin scaffold. In step 2, the functionalization of isolated curcuminoids with aromatic carbonitrile for the synthesis of novel curcumin analogues was carried out [49].

For the first step to isolate the three major curcuminoids from turmeric, 5g of turmeric (AR grade) was subjected to column chromatography using silica gel as the stationary phase (fig. 4, Scheme 1). As the elutant benzene/ethyl acetate were used, where an 82:18 elutant fraction separated out 70% of curcumin, a 70:30 elutant fraction separated out 68% of demethoxy curcumin, and a 54:48 elutant fraction gave 58% of bisdemethoxy curcumin [50].

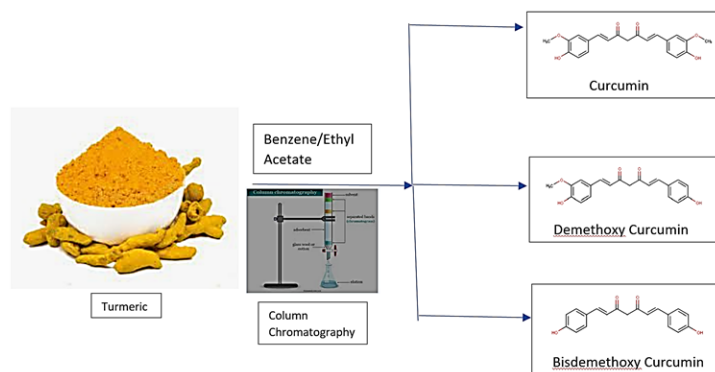


Fig. 4: Scheme1-Isolation of curcuminoids from turmeric powder

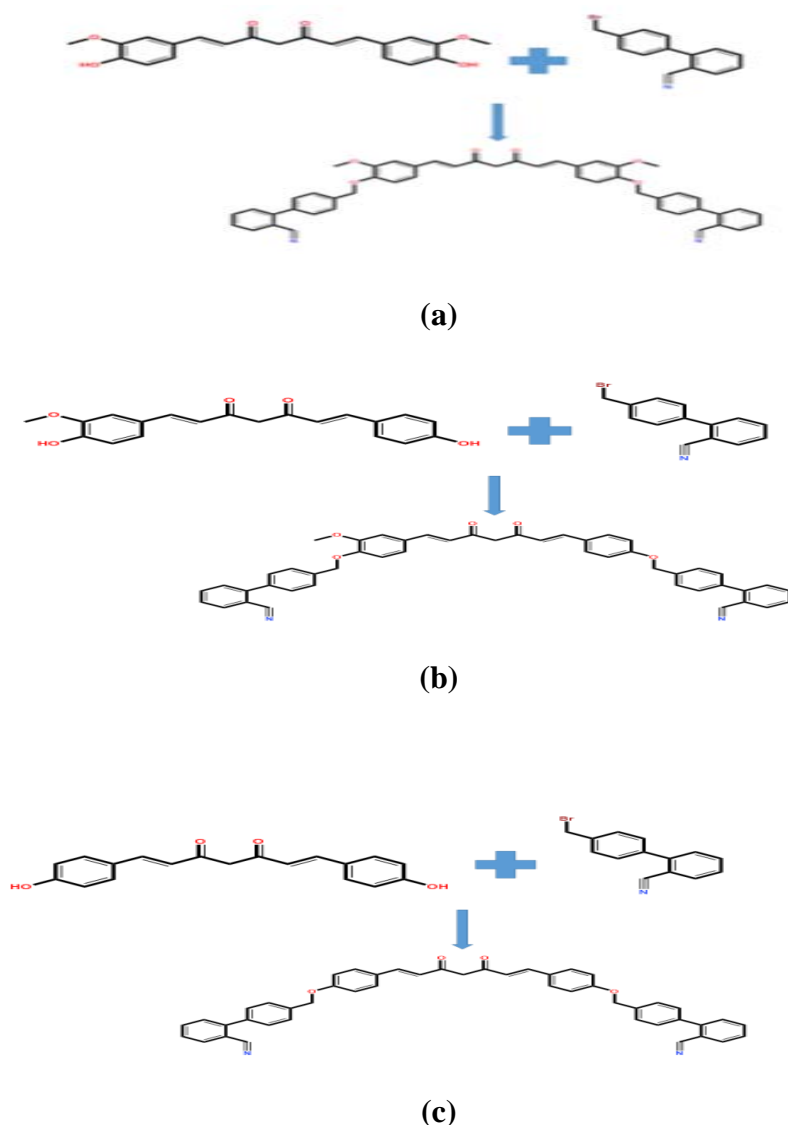


Fig. 5: Schematic plan for the synthesis of curcumin-biphenylcarbonitrile conjugate from curcuminoids

Step 2: Equimolar quantities of isolated curcuminoids and bromobiphenyl carbonitrile were mixed and refluxed for 10-12 h. Reactions were checked intermittently with TLC (Thin Layer Chromatography). The reaction mixture was then filtered through hyflow layers using suction. The solid was then separated from the hyflow using methanol and purified by recrystallization. Fig. 5 outlines the synthesis of key intermediates [51].

#### Characterization and stability

Synthesized curcumin analogues were sent for NMR analysis, IR analysis, and mass spectrographic analysis for structural determination. To conduct the stability test, a 0.1 g sample was used. A stability test was carried out under the heading of acid hydrolysis, base hydrolysis, thermal degradation, and photolytic degradation for

24 h, 1 mo, and 3 mo as per the standard procedure using a UV-VIS spectrophotometer [52, 53].

#### Anticancer activity by MTT assay

To evaluate the cytotoxicity efficacy of all synthesized curcumin analogues, a 3-(4, 5-dimethylthiazol-2-yl)-2, 5-diphenyltetrazolium bromide assay (MTT assay) was carried out on PANC1 cell lines [54].

The cells were seeded in a 96-well flat-bottom microplate and maintained at 37 °C with 95% humidity and 5% CO<sub>2</sub> overnight. The samples were treated with different concentrations (100, 50, 25, 12.5, 6.25, and 3.125 µg/ml). The cells were incubated for another 48 h. The wells were washed twice with phosphate-buffered saline solution (PBS) and then 20 µl of the MTT staining solution was added to each well and the plate was incubated at 37 °C. After 4 h, 100 µl of dimethyl sulfoxide (DMSO) was added to each well to dissolve the formazan crystals, and absorbance was recorded at 570 nm using a microplate reader. As a control, doxorubicin was used to compare the potency of each curcumin derivative. The absorbance of the culture medium without PANC1 cells was taken as blank, and it was subtracted. The vehicle control was the PANC1 cells treated with a suitable concentration of DMSO. IC<sub>50</sub> values (50% inhibition concentration of drug molecules) of novel drug molecules was calculated by using GraphPad Prism Version 5.1 software [54, 55].

The percentage of cell viability for each concentration considered was calculated by dividing the sample optical density (OD) by the control OD, i.e., Surviving cells (%) = Mean OD of test compound / Mean OD of Negative control × 100

## RESULTS AND DISCUSSION

### Molecular docking study

Table 2: Docking scores of the standard drugs and parent compounds

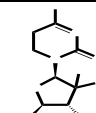
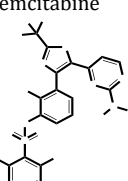
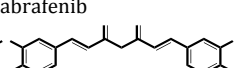
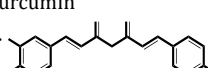
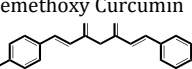
Parent compound	Docking score	Glide energy kcal/mol	H bond	Bond length (Å)
 Gemcitabine	-3.8	-32.428	Asp54 backbone Sidechain Leu6 backbone	2.22 2.24 1.93
 Dabrafenib	-3.546	-41.748	Glu62 Side Chain	1.68
 Curcumin	-2.555	-43.54	Thr35 backbone Asp54 sidechain	1.95 2.44
 Demethoxy Curcumin	-5.531	-49.973	Arginine154 Pi-cation Glycine 70 Backbone	6.43 2.54
 Bisdemethoxy Curcumin	-5.064	-49.367	GLH37 backbone	2.05

Table 3: Docking scores of newly designed curcumin derivatives

Structures	Docking scores	Glide energy (kcal/mol)	H bond	Bond length (Å)
CD2	-7.12	-68.66	Lysine147 Pi-cation Aspartic acid30 Salt bridge with nitrile	5.43 3.57
CD3	-7.05	-71.09	Lysine147 Pi-cation Lysine117 Pi-cation	5.31 4.51
CD1	-6.80	-62.73	Lysine147 Pi-cation Lysine 117 Pi-cation	5.21 4.50
CD5	-6.56	-67.02	Thr35-backbone Leu6-backbone	2.12 2.10

Both the commercial drugs, Gemcitabine and Dabrafenib, which are mainly used for the treatment of pancreatic cancer, have a pyrimidine ring and an amino group. The only distinction is that in Gemcitabine, the furan ring is linked to a pyrimidine ring, whereas in Dabrafenib, the thiazole ring is linked to an amino group is present on the pyrimidine ring of both gemcitabine and dabrafenib, respectively. There are additional groups attached to the thiazole ring of the Dabrafenib molecule, but in Gemcitabine, only fluorine and hydroxyl groups are attached to the furan ring.

In the 2D structure of target-ligand interaction for Gemcitabine, the presence of hydroxyl groups is noticed on the outwards and inwards of the furan ring. Among these hydroxyl groups, the hydroxyl attached to the furan ring shows interaction with two amino acids via a backbone hydrogen bond. These two amino acids are Asp54 of 2.24 Å and Leu6 of 1.93 Å bond length, respectively, whereas sidechain bond interaction with Asp54 (2.22 Å bond length) is observed with other hydroxyl groups. Here, Leu6, a nonpolar amino acid, is composed of an aliphatic R group, and Asp54 is an electrically charged amino acid containing a negatively charged R group along with carboxylate. It has been noticed that the glide score of Gemcitabine is -3.8 and the glide energy of Gemcitabine is -32.428 kcal/mol (table 2). In the 2D structure of the target-ligand interaction for Dabrafenib, a side chain hydrogen bond interaction is observed between amino groups present as a substituent on the pyrimidine ring and Glutamic acid 62 (Glu62) of the target protein (bond length of 1.68 Å). Glutamic acid 62 is an electrically charged amino acid containing a negatively charged carboxylate chain. The Dabrafenib glide score is -3.546 and the glide energy is -41.748 kcal/mol [49, 56].

CD4	-5.69	-60.93	Glu37-backbone	2.57
CD6	-5.62	-62.92	Thr35-backbone	1.89
CD9	-4.002	-58.99	-	-
CD8	-	-	-	-
CD7	-	-	-	-
CD2	-3.497	-37.131	Lysine 147 Pi-cation	5.23
			Lysine 117 Pi-cation	4.53
CD3	-1.439	-19.484	Lysine147 P-cation	5.95

The glide score and glide energy of curcumin are found to be -2.555 and -43.54, respectively. In curcumin, one hydroxyl group present on the phenyl ring shows backbone hydrogen bond interaction with Thr35 amino acid (1.95 Å bond length) and the other hydroxyl group shows side chain hydrogen bond interaction with Asp54 having a bond length of 2.44 Å. The binding affinity of Curcumin is similar to that of Gemcitabine.

### Designed curcumin derivatives

To design the nine novel curcumin analogues, without disturbing the alpha-beta diketone moiety, curcumin was subjected to structural modifications. The designed curcumin derivatives were docked with the KRAS protein target (PDB: 4EPV; fig. 3). The docking scores of nine designed curcumin derivatives are illustrated in table 3 in descending order.

The docking scores of the newly designed derivatives reveal that the curcumin analogues show strong interactions with the target protein. In the ligand interaction images of the newly designed curcumin analogues, for most of the curcumin analogues, pi-cation interaction is observed with several amino acids such as Lysine147, Lysine117, backbone H-bond with Glutamic acid 37, Aspartic acid 38, Threonine 35, and Leucine 6, as well as salt bridges with Aspartic acid 30. This confirms that newly designed curcumin analogues are capable of binding inside the pocket of the target protein [57, 58].

Compared to Curcumin and Bisdemethoxy Curcumin (-2.555 and 5.064), the docking score of Demethoxy Curcumin is -5.531, demonstrating the strongest binding affinity. Pi-cation interactions with Arginine 154 (6.43 Å bond length) and Glycine 70 (2.54 Å bond length) are depicted in 2D and 3D frames with backbone hydrogen interaction.

Docking scores in table 3 suggest that among all nine newly designed curcumin analogues, three curcumin derivatives, CD1, CD2, and CD3, display better docking scores than other designed derivatives, therefore, they are identified as hit molecules. This revealed their inability to fit into the pocket of the target. Other designed curcumin derivatives with low docking scores are able to fit into the pocket of the target protein via different interactions like Vander Vaal's forces, hydrophobic interactions etc. whereas CD7 and CD8 did not exhibit any docking scores.

The nitrile moiety present in CD2 shows a salt bridge with Aspartic acid 30, having a bond length of 3.57 Å. CD2 glide energy (-68.66 kcal/mol) is significantly lower than that of the standard commercial drugs Gemcitabine (-32.428 kcal/mol) and Dabrafenib (-41.748 kcal/mol). This indicates that CD2 has the potential for tight binding with the target. CD2 also shows a conformer with a docking score of -3.497 and glide energy of -37.131. Pi-cation interactions are seen with Lysine 147 and Lysine 117 having a bond length of 5.23 Å and 4.53, Å respectively (fig. 6).

### CD2

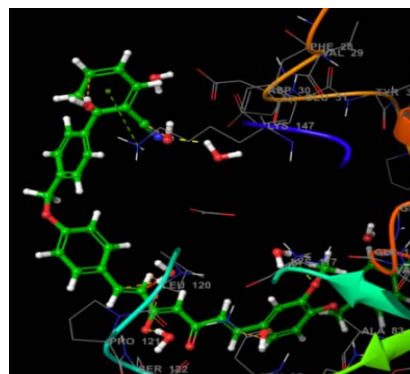
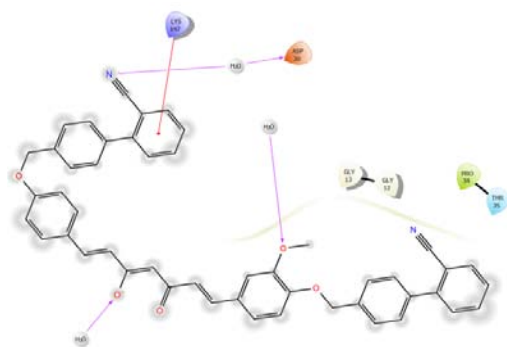


Fig. 6: Molecular docking model of CD2 with 4EPV-2D interaction map for CD2 docking with 4EPV and 3D model

### CD3

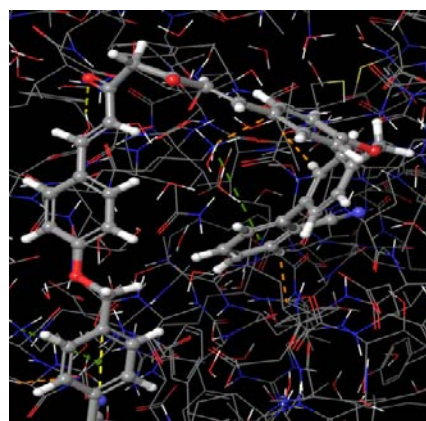
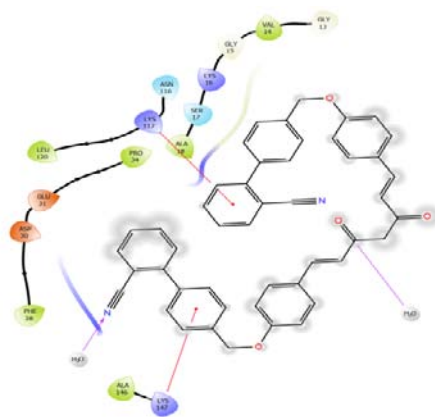
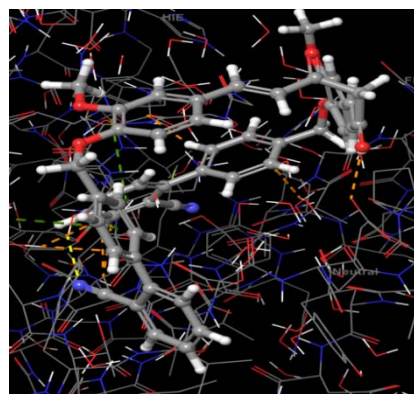
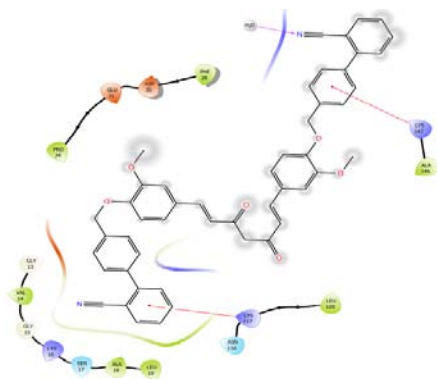


Fig. 7: Molecular docking model of CD3 with 4EPV-2D interaction map for docking of CD3 with 4EPV and 3D model

CD1



**Fig. 8: Molecular docking model of CD1 with 4EPV-2D interaction map for docking of CD1 with 4EPV and 3D model**

The phenyl ring attached to the carbonitrile shows pi-cation interaction with Lysine 117 (bond length 4.51Å) and Lysine 147 (bond length 5.31 Å). The glide energy of CD3 (-71.09 kcal/mol) is better than the commercial drugs Gemcitabine (-32.428 kcal/mol) and Dabrafenib (-41.748 kcal/mol), which suggests the similarity in binding mode of the novel synthesized molecule (CD3) with the target protein. The conformer of CD3 has a docking score of -1.439 and glide energy of -19.484 kcal/mol, respectively. The phenyl ring of curcumin shows pi-cation interaction with Lysine 147, having a bond length of 5.95Å (fig. 7).

The docking score of CD1 is -6.80 and the glide energy is -62.73 kcal/mol. The phenyl ring attached to the carbonitrile shows pi-cation interaction with Lysine 117 (bond length 4.50Å) and Lysine 147 (bond length 5.21Å) (fig. 8). The glide energy of this derivative (-59.404 kcal/mol) is better than the standard drugs Gemcitabine (-32.428 kcal/mol), Dabrafenib (-41.748 kcal/mol), which gives an idea of the strong binding of CD1 with the target protein KRAS [59].

#### ADMET prediction

To predict pharmacokinetic parameters such as ADMET using an *in silico* method, an ADMET study was planned in the first stage itself to investigate the nature of novel drug molecules to avoid wasting time on hit candidate/s that may be toxic or incompetent to cross cell membranes or metabolized in the human body in an inactive form. In the present work, various physicochemical properties of all three hit molecules (CD1, CD2, and CD3) were calculated and are summarized in tables 4 and 5.

Through the Swiss ADME [59-61] analysis, it was perceived that all three novel drug molecules (CD1, CD2, and CD3) do not follow the Lipinski's rule of five towards drug-likeness with respect to molecular weight and MLogP/WLOGP. They have 2 or more than 2 violations, which suggests that they are not orally active derivatives. The results of the Swiss ADME tool indicate that synthesized curcumin derivatives are not very bioavailable for oral administration either. Moreover, all three synthesized molecules violate Egan's rule as their lipophilicity values (n-octanol/water partition coefficient) are greater than 5.88, although the topological polar surface area is within the given limits. Overall, from the drug-likeness results, all three synthesized curcumin derivatives moderately possess a drug-like nature.

The AdmetLab 2.0 was used to assess the cell permeability of the novel drug molecule (Caco-2 cell) [58]. As per the obtained data, only CD3 has the ability to penetrate the Caco cell while CD2 is on the margin. The blood-brain barrier and CNS activity are equally important to be considered when the drug is acting peripherally. Negative values express that the drug has poor blood-brain barrier permeability, while positive values (>0.3) indicate good permeation. Based on these parameters, results suggest that the synthesized curcumin derivatives have low BBB permeability, although all three are capable of penetrating the central nervous system as CNS permeability is within the limit. Drug metabolism was estimated based on the Cytochrome P450 (CYP) models

(CYP1A2, CYP2C19, CYP2C9, CYP2D6, and CYP3A4) for substrate or inhibition. All the synthesized curcumin analogues are found to be inhibitors of CYP1A2 enzyme, CYP2C19 enzyme, CYP2C9 enzyme, and CYP3A4 enzyme, which leads to decreased metabolism of substrate drugs, whereas they are non-inhibitors of CYP2D6 enzyme. According to the Clearance (CL) results in table 5, the clearance level for all three chemical entities is between 5 and 15 ml/min/Kg. It concludes that novel drug molecules have an adequate clearance rate. They also have a shorter half-life. All three drug molecules act as hERG I and II inhibitors and exhibit hepatotoxicity, which means they can cause liver damage and thus have liver toxicity. Ames test turns out to be positive for all the synthesised derivatives; hence, all three synthesised chemical molecules are mutagenic and can cause mutations in the DNA.

#### Synthesis

For the synthesis of curcumin analogues conjugated with a pharmacophore-biphenyl carbonitrile moiety, the reaction was carried out in two steps [60-62]. The yield of all three synthesized curcumin derivatives conjugated with aromatic carbonitrile (CD1, CD2 and CD3) was good enough for further studies. The percentage yield of curcumin derivatives was about 70% w/w, while that of demethoxy curcumin derivative was about 68% w/w and that of bisdemethoxy curcumin derivative was about 58% w/w [59, 63].

#### Characterization

FTIR results show characteristic peaks between 1275  $\text{cm}^{-1}$ -1200  $\text{cm}^{-1}$ , which signify the presence of ether linkage. Multiple peaks in CD1 indicate that more than one ether linkage is present, including the methoxy group of curcumin and a link between biphenyl carbonitrile and curcumin. Whereas a single characteristic peak at 1272  $\text{cm}^{-1}$  in CD2 and CD3 implies that only one kind of ether linkage is present that might be between biphenyl carbonitrile and curcumin. Sharp peaks at 1627  $\text{cm}^{-1}$  and 1594  $\text{cm}^{-1}$  confirm the presence of the diketo group, and the characteristic peak of benzene is visible at 1906  $\text{cm}^{-1}$ . Distinct peaks corresponding to 3023  $\text{cm}^{-1}$  and 2992  $\text{cm}^{-1}$  represent the C-H stretching vibrations of the biphenyl ring and strong peaks at 2221  $\text{cm}^{-1}$  and 2220  $\text{cm}^{-1}$  validate the presence of the cyano group in all the three synthesized novel curcumin analogues (CD1, CD2 and CD3, fig. 9a-c) [63, 64].

#### CD1

$^1\text{H}$  NMR of CD1 in DMSO:  $\delta$ -3.8 (s 6H,  $\text{OCH}_3$  of Curcumin),  $\delta$ -4.8 (2H methylene between diketo group),  $\delta$ -6.7 to  $\delta$ -7.6 (aromatic H).  $^1\text{H}$  NMR  $\delta$  7.97 (d, 2H,  $J=8.71$  Hz, biphenyl ring),  $\delta$  (ppm): 7.79 (d,  $J=7.2$  Hz, 2H), 7.62 (t,  $J=3.6$  Hz, 1H), 7.56-7.59 (m, 3H), 7.52 (d,  $J=7.6$  Hz, 1H), 7.32 (m, 2H)] [Curcumin 6.06 (s, 1H), 6.77 (d, 2H), 7.56 (d, 2H), 7.32, 6.83, 7.16, (s, 3H)] [65]. Further confirmation was done by finding the mass using LC-MS and comparing it with the calculated one. LC/MS (m/z) calculated: 750.84, while graph shows 751.58 (fig. 10a-b).



Table 4: Drug likeness and *in silico* molecular properties of CD1, CD2 and CD3

Parameters	Standard value	CD1	CD2	CD3
Lipinski's Rule	Yes; 0 violation	No; 2 violations: MW>500, MLOGP>4.15	No; 2 violations: MW>500, MLOGP>4.15	No; 2 violations; MW>500, MLOGP>4.15
MW (Molecular weight)	<500	736.81g/mol	706.78 g/mol	676.76 g/mol
MLogP (Moriguchi octanol-water partition coefficient)	≤4.15	4.19	4.55	4.92
nHBA (number of H-bond acceptor)	≤10	8	7	6
nHBD (number of H-bond donor)	≤5	0	0	0
Egan's Rule	Yes; 0 violation	No; 1 violation: WLOGP>5.88	No; 1 violation: WLOGP>5.88	No; 1 violation: WLOGP>5.88
WLOGP (Lipophilicity; n-octanol/water partition coefficient)	≤5.88	10.04	10.03	10.02
TPSA (Topological Polar Surface Area)	≤131.6 Å <sup>2</sup>	118.64 Å <sup>2</sup>	109.41 Å <sup>2</sup>	100.18 Å <sup>2</sup>
Bioavailability Score	0.55	0.17	0.17	0.17

Table 5: ADMET studies of CD1, CD2 and CD3.

Parameters	Standard value	CD1	CD2	CD3
<b>Adsorption</b>				
Caco-2 Permeability	Optimal condition: higher than -5.15 Log unit	-5.17	-5.156	-5.143
Pgp (P-glycoprotein) substrate	Yes-substrate; No-non-substrate	Yes	Yes	Yes
Pgp (P-glycoprotein) I inhibitor	Yes-substrate; No-non-substrate	Yes	Yes	Yes
Pgp (P-glycoprotein) II inhibitor	Yes-substrate; No-non-substrate	Yes	Yes	Yes
<b>Distribution</b>				
BBB (Blood Brain Barrier); Permeability (log BB)	Log BB>0.3 (high); Log BB<-1 (poor)	-3.681 (BBB-)	-3.761 (BBB-)	-3.651 (BBB-)
CNS (Central Nervous System) Permeability (log PS)	Log PS>-2 (penetrate); Log PS<-3 (difficult to penetrate)	-2	-2	-2
VDss human (Volume of Distribution)	Log VDss>0.45 (high); Log VDss<-0.15 (low)	-0.136	-0.188	-0.327
<b>Metabolism</b>				
CYP1A2 enzyme	Yes-inhibitor; No-non-inhibitor	Yes	Yes	Yes
CYP2C19 enzyme	Yes-inhibitor; No-non-inhibitor	Yes	Yes	Yes
CYP2C9 enzyme	Yes-inhibitor; No-non-inhibitor	Yes	Yes	Yes
CYP2D6 enzyme	Yes-inhibitor; No-non-inhibitor	No	No	No
CYP3A4 enzyme	Yes-inhibitor; No-non-inhibitor	Yes	Yes	Yes
<b>Excretion</b>				
CL	High: >15 ml/min/Kg; moderate: 5-15 ml/min/Kg; low: <5 ml/min/Kg	8.274	7.755	6.099
T <sub>1/2</sub>	1: long half-life; 0: short half-life	0.032	0.013	0.008
<b>Toxicity</b>				
Hepatotoxicity	Yes-inhibitor; No-non-inhibitor	Yes	Yes	Yes
hERG I inhibitor	Yes-inhibitor; No-non-inhibitor	Yes	Yes	Yes
hERG II inhibitor	Yes-inhibitor; No-non-inhibitor	Yes	Yes	Yes
Ames Test	0-0.3: excellent; 0.3-0.7: medium; 0.7-1.0: poor	Positive (0.692)	Positive (0.653)	Positive (0.645)

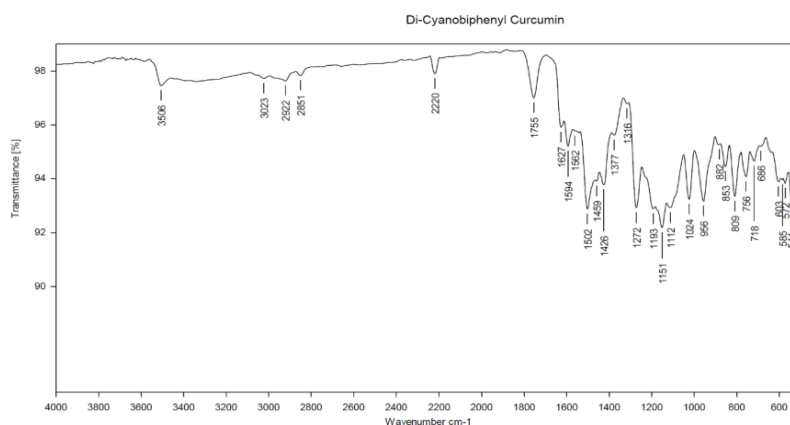
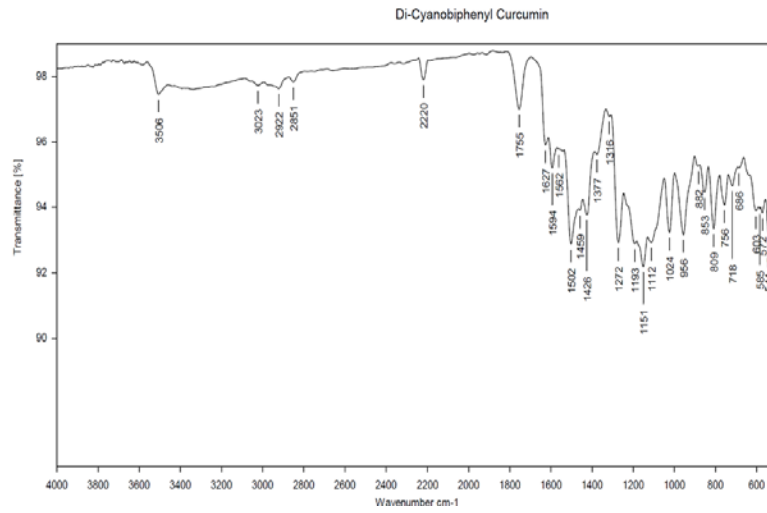
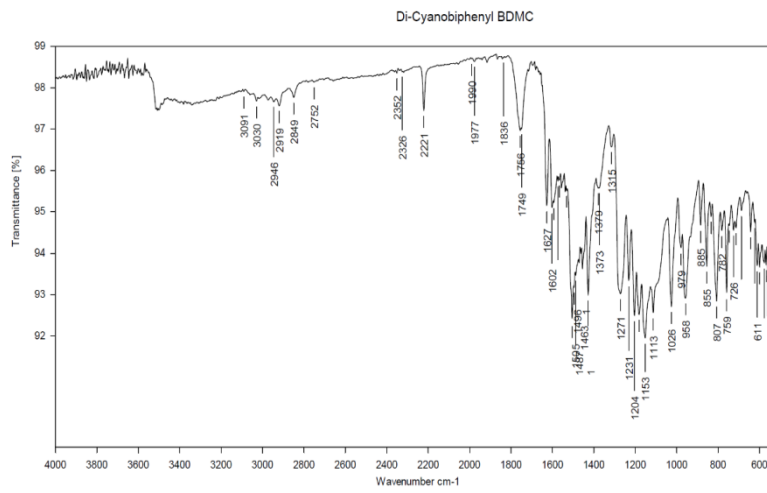


Fig. 9a: IR graph of CD1



**Fig. 9b: IR graph of CD2**



**Fig. 9c: IR graph of CD3**

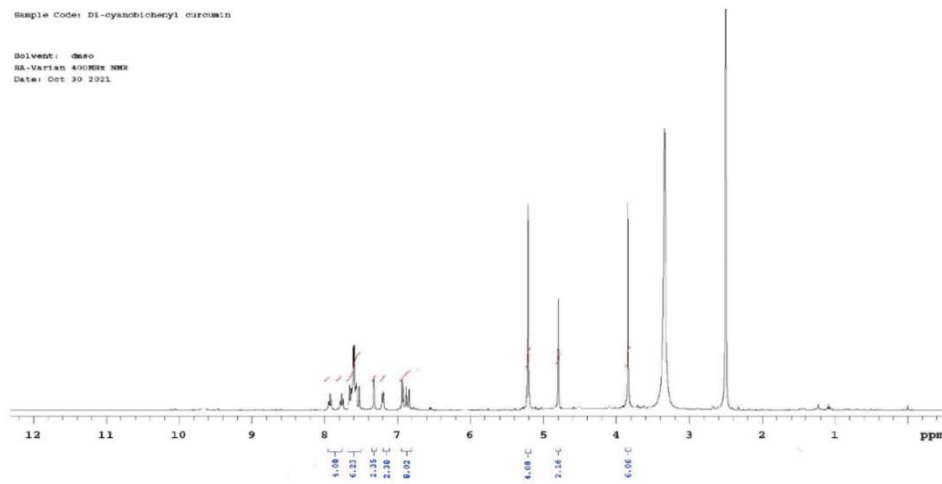


**Fig. 10a: NMR graph of CD1 in DMSO**

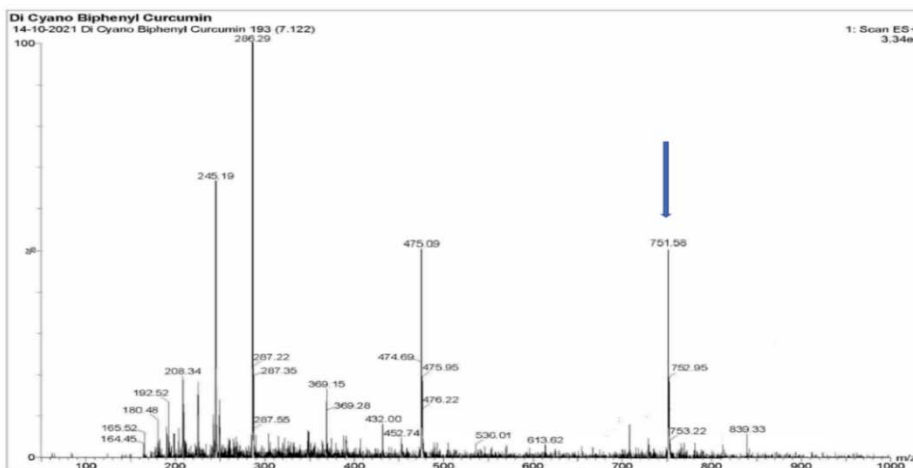


Fig. 10b: LC/MS of CD1

CD2

<sup>1</sup>H NMR: δ-3.8 (s 3H, OCH<sub>3</sub> of Curcumin), δ-4.8 (2H methylene between diketo group), δ=6.7 to δ=7.6 (aromatic H). <sup>1</sup>H NMR δ 7.97 (d, 2H, J=8.71 Hz, biphenyl ring), δ (ppm): 7.79 (d, J = 7.2 Hz, 2H), 7.62 (t, J = 3.6 Hz, 1H),

7.56–7.59 (m, 3H), 7.52 (d, J = 7.6 Hz, 1H), 7.32 (m, 2H) [Curcumin 6.06 (s, 1H), 6.77 (d, 2H), 7.56 (d, 2H), 7.32, 6.83, 7.16, 3.84 (s, 3H)] [63]. The structure of synthesized CD1 was further confirmed by mass spectrograph [65]. The calculated LC/MS (m/z) of CD2 is 720.84, whereas the LC/MS graph shows 720.49 (fig. 11a-b) [65].

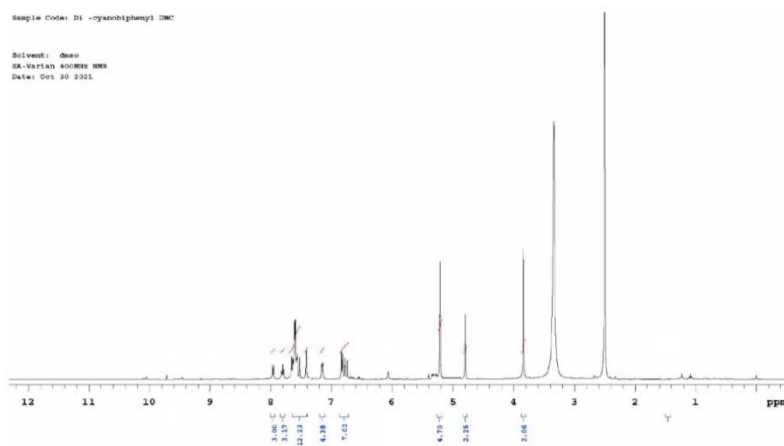


Fig. 11a: NMR graph of CD2 in DMSO

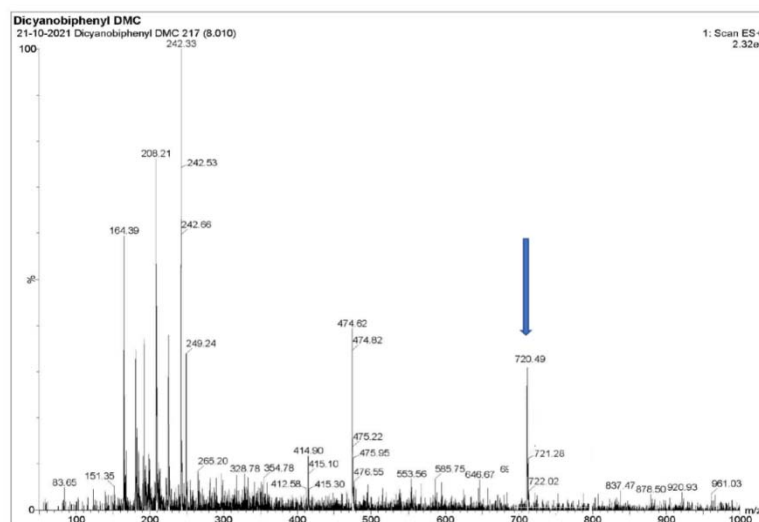


Fig. 11b: LC/MS of CD2

**CD3**

$^1\text{H}$  NMR  $\delta$  (ppm): As the peak at  $\delta$ -3.8 Hz is absent in this graph but present in the graphs of curcumin derivative and demethoxy curcumin derivative confirms the absence of  $\text{OCH}_3$  in this derivative

7.95 (d, 2H,  $J$ =8.71 Hz, biphenyl ring), 7.82 (d, 2H,  $J$ =8.65 Hz, biphenyl ring), 7.66 (d, 2H,  $J$ =8.84 Hz, Ar-CH), 7.56 (d, 2H,  $J$ =8.47 Hz, Ar-CH), 7.32 (d, 2H,  $J$ =8.51 Hz, biphenyl ring), 6.83 (d, 2H,  $J$ =8.83 Hz, biphenyl ring), 4.79 (t, 2H,  $J$ =5.70 Hz,  $\text{CH}_2\text{-O}$ ) [63]. Calculated LC/MS ( $m/z$ ): 690.78, while from the graph, it is 691.40 (fig. 12a-b) [65].

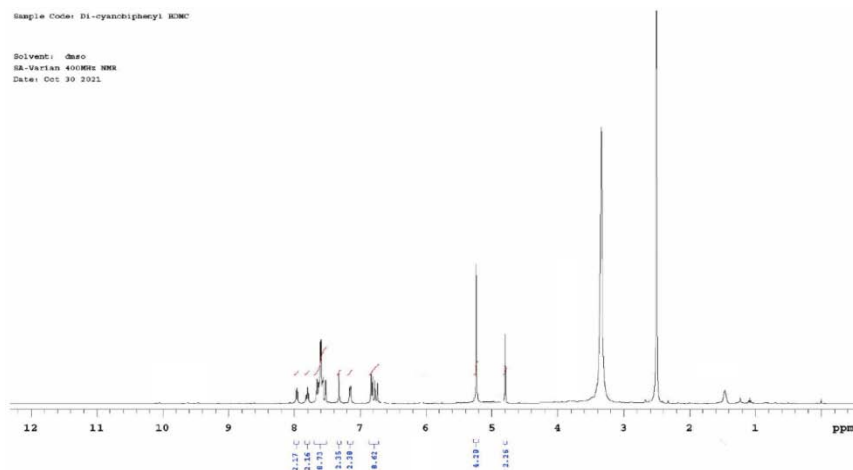


Fig. 12a: NMR graph of CD3 in DMSO

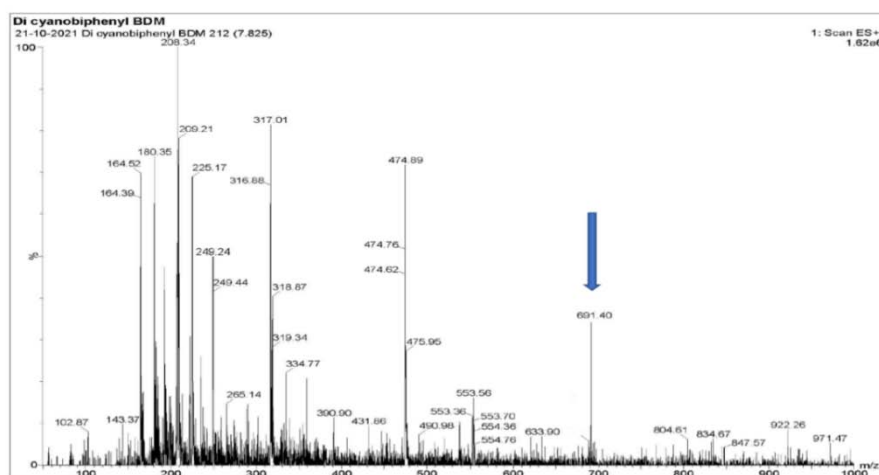


Fig. 12b: LC/MS of CD3

**Stability**

Stability studies of synthesized drug molecules are crucial to interpret the implications of the degraded products of new drug molecules on human health. Furthermore, it may provide useful information about how long these drug molecules can retain their

health benefits. Stability tests for all three molecules (CD1, CD2 and CD3) were done by UV-VIS Spectrophotometer and it was found that all three derivatives were stable for a period of 24 h and a period of 1 mo, while after a period of three months, slight degradation is seen, which requires further analysis to confirm. (fig. 13a-d, 14a-d, and 15a-d) [50].

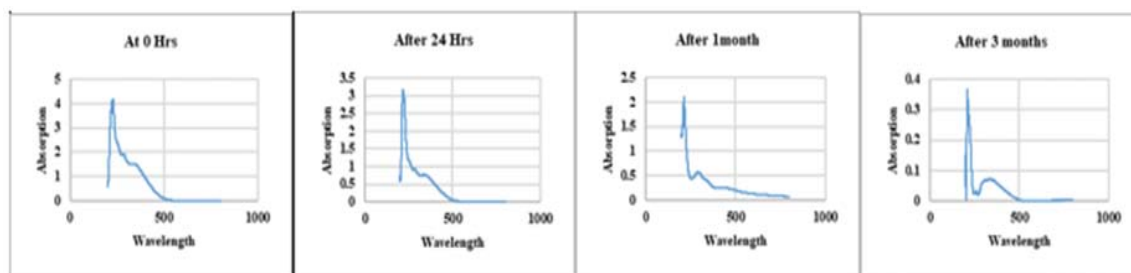
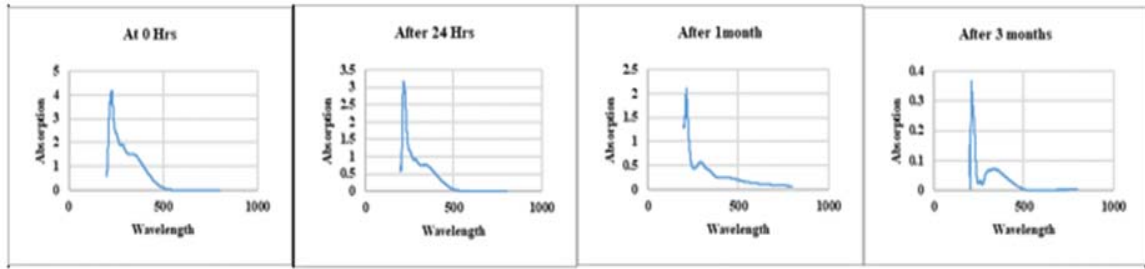
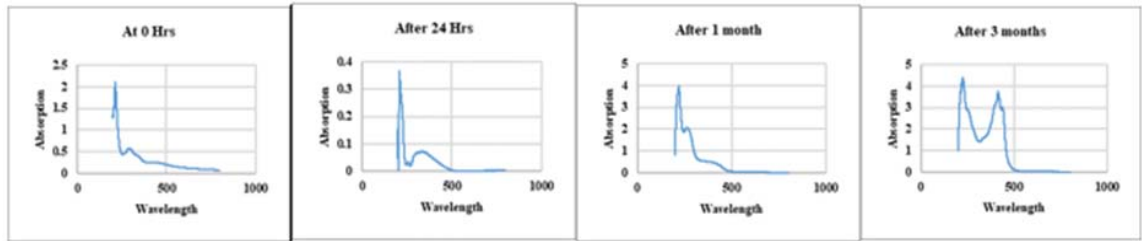
**Stability results of CD1**

Fig. 13a: Acid hydrolysis of CD1



**Fig. 13b: Base hydrolysis of CD1**



**Fig. 13c: Photolytic degradation of CD1**

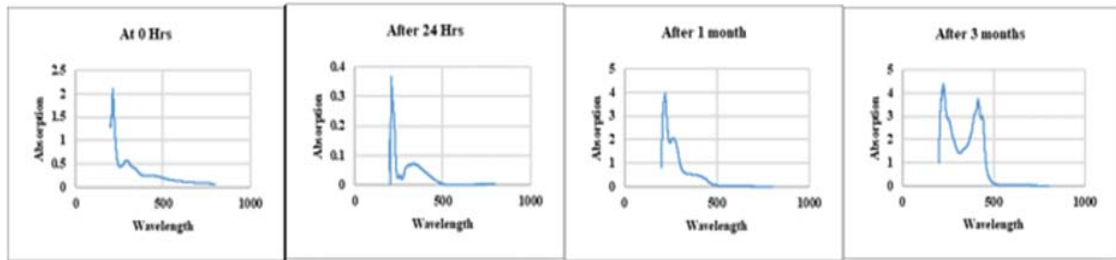


**Fig. 13d: Thermolytic degradation of CD1**

**Stability results of CD2**

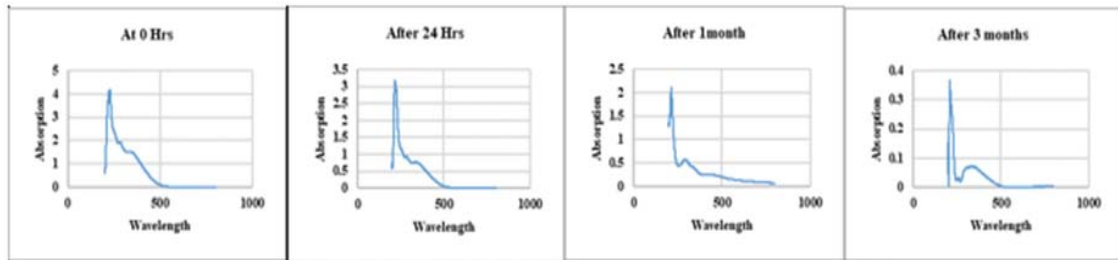


**Fig. 14a: Acid hydrolysis of CD2**

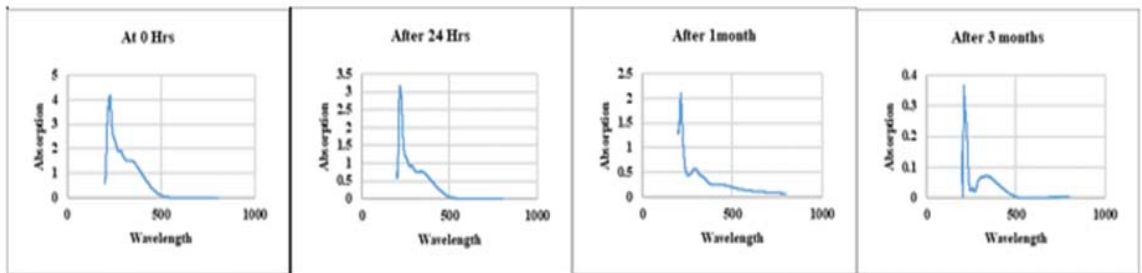


**Fig. 14b: Base hydrolysis of CD2**

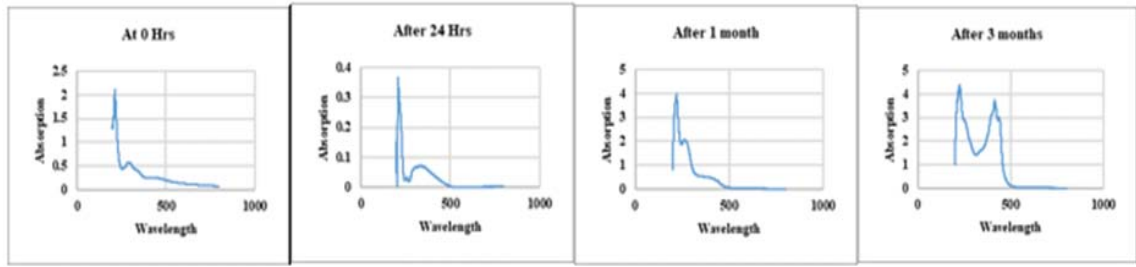


**Fig. 14c: Photolytic degradation of CD2**

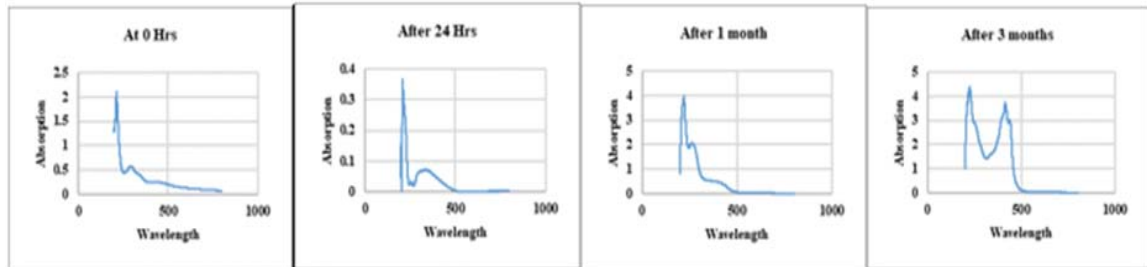


**Fig. 14d: Thermolytic degradation of CD2**

**Stability results of CD3**

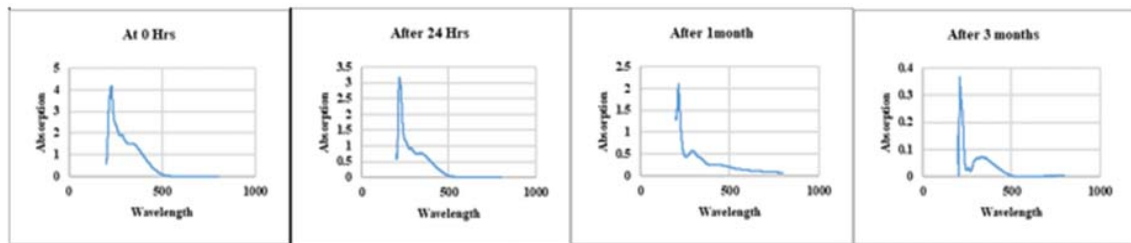


**Fig. 15a: Acid hydrolysis of CD3**

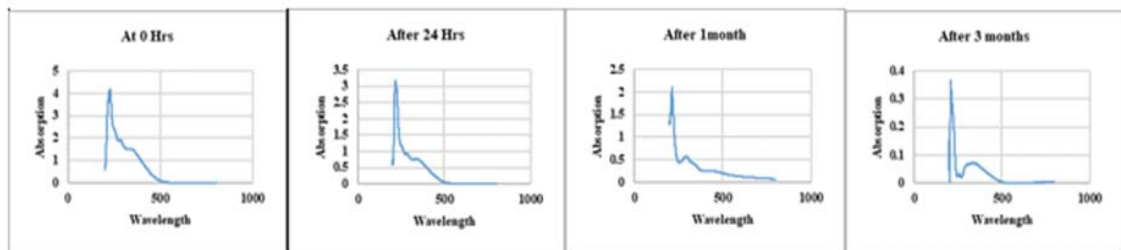


**Fig. 15b: Base hydrolysis of CD3**

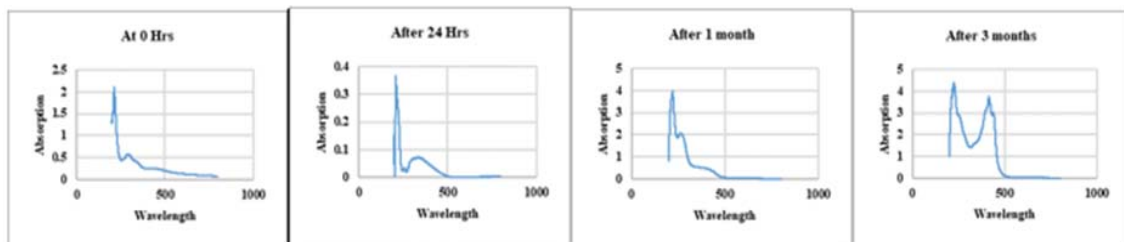


**Fig. 15c: Photolytic degradation of CD3**

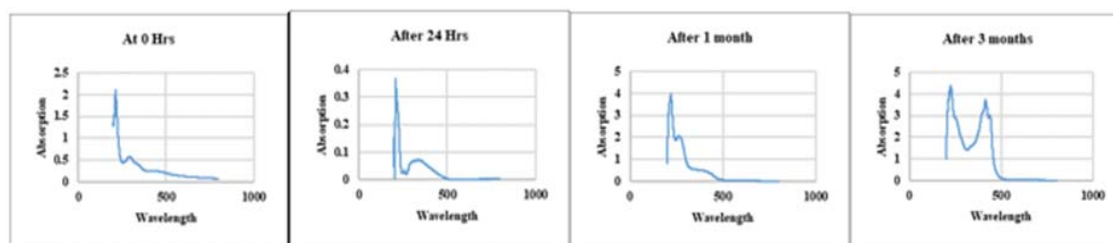


Fig. 15d: Thermolytic degradation of CD3

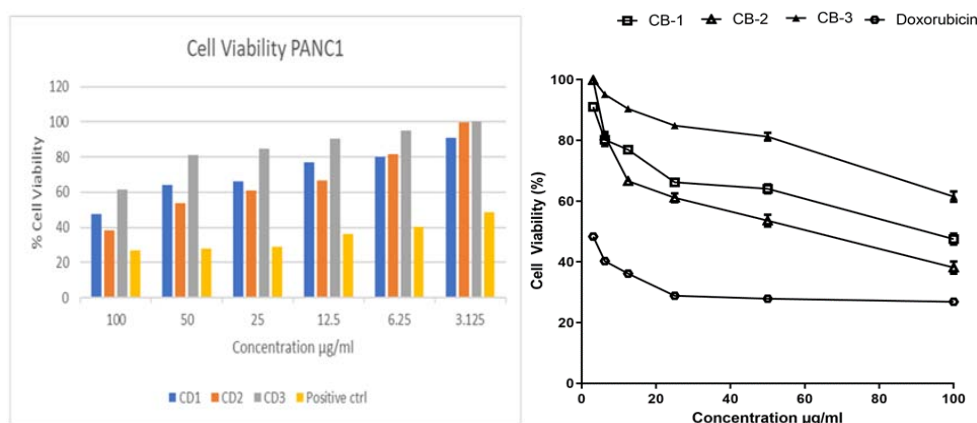


Fig. 16: Cell viability percentage of CD1, CD2 and CD3 against PANC1 cell line

### Anticancer activity by MTT assay

The anti-proliferative activity of CD1, CD2, and CD3 was evaluated by MTT assay on PANC 1 cells. Results were compared with positive control (Doxorubicin). IC<sub>50</sub> values of all three curcumin derivatives were found to be 168.60 (µg/ml) for CD3, 45.27 (µg/ml) for CD2 and for CD1 it was 67.51 (fig. 16). Better anticancer activity might be due to the presence of the nitrile groups (-CN) which are usually reported to have enhanced the activity [65].

Calculated values of IC<sub>50</sub> are quite eloquent and suggest that CD2 possesses better potency than the other derivatives. At the concentration of 100 µg/ml the cell viability percentage is reduced to 38.1%, which is quite close to Doxorubicin (26.8%) used as a positive control. Therefore, the synthesized curcumin derivatives do inhibit the proliferation of cells and hence exhibit anticancer activity against PANC1 cell lines. Although as per the available data, synthesized curcumin derivatives are demonstrated to inhibit the proliferation of cells, there is a scope of structural modifications to enhance their anticancer efficacy against the PANC1 cell line [65].

### CONCLUSION

In our previous work, we reported that synthesized novel curcumin derivatives with a tetrazole motif were verified to be active on PANC1 cell lines. In continuation of research work, a series of curcumin and aromatic carbonitrile were designed (CD1 to CD9). Present paper reports, for the first time, the synthesis and anticancer activity of three new hybrid molecules (CD-1, CD-2, and CD-3) as biphenylcarbonitrile-curcumin conjugates with high yield. ADMET studies suggest that all three synthesized drug molecules have cell permeability. Available ADMET data of novel curcumin analogues recommend their lipophilic nature with low bioavailability, indicating their amiss nature for oral adsorption. ADMET data confirm their low BBB permeability, although all three are capable of penetrating the central nervous system. All the synthesised curcumin analogues are found to be inhibitors of the

CYP1A2 enzyme, CYP2C19 enzyme, CYP2C9 enzyme, and CYP3A4 enzyme, which leads to decreased metabolism of substrate drugs.

Stability studies corroborate the stability of all three synthesized curcumin derivatives in the given conditions, although slight changes were seen after a 3-month period, which requires further investigation. The IC<sub>50</sub> values of all three curcumin derivatives, 168.60 (µg/ml) @ CD3, 45.27 (µg/ml) @ CD2 and 67.51 @ CD1, are quite eloquent. Taken together, all these findings imply biphenylcarbonitrile-curcumin analogues as excellent "lead anticancer molecules" against PANC I cells. This study has opened the doors to new findings and can be used as a template work, which may be very useful in smart drug discovery for the treatment of pancreatic cancer.

### ACKNOWLEDGEMENT

This work was partially funded by Karnataka Science and Technology Academy (KSTA), Department of Science and Technology, Government of Karnataka, India. Authors are thankful to M. S. Ramaiah University of Applied Sciences, Bangalore, India for giving us the opportunity to carry out this research work.

### AUTHORS CONTRIBUTIONS

All the authors have contributed equally.

### CONFLICT OF INTERESTS

Declared none

### REFERENCES

1. American Society of Clinical Oncology. The state of cancer care in America, 2014: a report by the American Society of Clinical Oncology. J Oncol Pract. 2014 Mar;10(2):119-42. doi: 10.1200/JOP.2014.001386, PMID 24618075.
2. Torre LA, Bray F, Siegel RL, Ferlay J, Lortet Tieulent J, Jemal A. Global cancer statistics, 2012. CA Cancer J Clin. 2015 Mar;65(2):87-108. doi: 10.3322/caac.21262, PMID 25651787.

3. Erratum to "Cancer statistics, 2021". CA Cancer J Clin. 2021;71(4):359. doi: 10.3322/caac.21669. PMID 34232515.
4. Taipale J, Beachy PA. The hedgehog and wnt signalling pathways in cancer. Nature. 2001 May 17;411(6835):349-54. doi: 10.1038/35077219, PMID 11357142.
5. Hanahan D, Weinberg RA. Hallmarks of cancer: the next generation. Cell. 2011 Mar 4;144(5):646-74. doi: 10.1016/j.cell.2011.02.013, PMID 21376230.
6. Rhett JM, Khan I, O'Bryan JP. Biology, pathology, and therapeutic targeting of RAS. Adv Cancer Res. 2020;148:69-146. doi: 10.1016/bs.acr.2020.05.002. PMID 32723567.
7. Eser S, Schnieke A, Schneider G, Saur D. Oncogenic KRAS signalling in pancreatic cancer. Br J Cancer. 2014 Aug 26;111(5):817-22. doi: 10.1038/bjc.2014.215, PMID 24755884.
8. Lu H, Marti J. Long-lasting salt bridges provide the anchoring mechanism of oncogenic Kirsten Rat sarcoma proteins at cell membranes. J Phys Chem Lett. 2020 Nov 19;11(22):9938-45. doi: 10.1021/acs.jpcl.0c02809. PMID 33170712.
9. Dracham CB, Shankar A, Madan R. Radiation induced secondary malignancies: a review article. Radiat Oncol J. 2018 Jun;36(2):85-94. doi: 10.3857/roj.2018.00290, PMID 29983028.
10. De AK, Bera T. Analytical method development, validation and stability studies by RP-HPLC method for simultaneous estimation of andrographolide and curcumin in co-encapsulated nanostructured lipid carrier drug delivery system. Int J App Pharm. 2021;13(5):73-86. doi: 10.22159/ijap.2021v13i5.42181.
11. Krishnamurthy G, Roy D, Kumar J. Curcumin, a natural golden drug and its anticancer aspects from synthesis to delivery: a review. Int J App Pharm. 2020;12(5):70-84. doi: 10.22159/ijap.2020v12i5.38586.
12. Heydari P, Zargar Kharazi A, Asgary S, Parham S. Comparing the wound healing effect of a controlled release wound dressing containing curcumin/ciprofloxacin and simvastatin/ciprofloxacin in a rat model: A preclinical study. J Biomed Mater Res A. 2022 Feb;110(2):341-52. doi: 10.1002/jbm.a.37292. PMID 34378857.
13. Kabir MT, Rahman MH, Akter R, Behl T, Kaushik D, Mittal V. Potential role of curcumin and its nanoformulations to treat various types of cancers. Biomolecules. 2021 Mar 7;11(3):392. doi: 10.3390/biom11030392, PMID 33800000.
14. Pandya N, Khan E, Jain N, Satham L, Singh R, Makde RD. Curcumin analogs exhibit anti-cancer activity by selectively targeting G-quadruplex forming c-myc promoter sequence. Biochimie. 2021 Jan;180:205-21. doi: 10.1016/j.biochi.2020.11.006. PMID 33188859.
15. Borgio JF, Bency BJ, Thorat PK, Lonkar AD. Gynandropsis pentaphylla DC extracts on the production of microbial proteins. Am J Drug Discov Dev. 2011;1(2):129-36. doi: 10.3923/ajdd.2011.129.136.
16. Krishnamurthy G, Deepti Roy L, Kumar J, Gour P, Arland SE, Prabu M. Study of in silico admet, molecular docking, and stability potential of synthesized novel tetrazole bearing curcumin derivatives and evaluation of their anticancer potential on panc-1 cell lines. Rasayan J Chem. 2023;16(1):335-54. doi: 10.31788/RJC.2023.1618114.
17. Mohamed SF, Flefel EM, Amr G, Abd El-Shafy DN. Anti-HSV-1 activity and mechanism of action of some new synthesized substituted pyrimidine, thiopyrimidine and thiazolopyrimidine derivatives. Eur J Med Chem. 2010 Apr;45(4):1494-501. doi: 10.1016/j.ejmech.2009.12.057, PMID 20110135.
18. Roy LD. Novel resveratrol analogues with aromatic hetero moieties: designing, one-pot synthesis and *in vitro* biological evaluation. Farmacia. 2023;71(1):130-43. doi: 10.31925/farmacia.2023.1.16.
19. Priyanka R, Lairikyengbam Roy VK, Manikanda P, Geeta K, Pooja G, Shivanjali A. Synthesis, characterization, and biological activity of novel azole piperazine congeners. J Appl Pharm Sci. 2023 Mar;13(04):53-69.
20. Rida SM, Ashour FA, El-Hawash SA, ElSemaary MM, Badr MH, Shalaby MA. Synthesis of some novel benzoxazole derivatives as anticancer, anti-HIV-1 and antimicrobial agents. Eur J Med Chem. 2005 Sep;40(9):949-59. doi: 10.1016/j.ejmech.2005.03.023, PMID 16040162.
21. Seth K, Garg SK, Kumar R, Purohit P, Meena VS, Goyal R. 2-(2-arylphenyl)benzoxazole as a novel anti-inflammatory scaffold: synthesis and biological evaluation. ACS Med Chem Lett. 2014 Feb 17;5(5):512-6. doi: 10.1021/ml400500e, PMID 24900871.
22. Angajala G, Subashini R. Synthesis, molecular modeling, and pharmacological evaluation of new 2-substituted benzoxazole derivatives as potent anti-inflammatory agents. Struct Chem. 2020;31(1):263-73. doi: 10.1007/s11224-019-01374-1.
23. Anusha P, Rao JV, Mohan GK. A review on diverse biological activities of benzoxazole molecule. World J Pharm Pharm Sci. 2017 May 18;6(7):1779-94.
24. Singh S, Veeraswamy G, Bhattarai D, Goo JI, Lee K, Choi Y. Recent advances in the development of pharmacologically active compounds that contain a benzoxazole scaffold. Asian J Org Chem. 2015 Dec;4(12):1338-61. doi: 10.1002/ajoc.201500235.
25. Correction to Lancet Respir Med 2020. Lancet Respir Med. 2020 Apr;8(4):e26:30079-5. doi: 10.1016/S2213-2600(20)30103-X.
26. Cram DJ. The design of molecular hosts, guests, and their complexes (Nobel lecture). Angew Chem Int Ed Engl. 1988 Aug;27(8):1009-20. doi: 10.1002/anie.198810093.
27. Kelloff GJ, Lubet RA, Lieberman R, Eisenhauer K, Steele VE, Crowell JA. Aromatase inhibitors as potential cancer chemopreventives. Cancer Epidemiol Biomarkers Prev. 1998 Jan;7(1):65-78. PMID 9456245.
28. Singh H, Walker AJ, Amiri Kordestani L, Cheng J, Tang S, Balcazar P. US food and drug administration approval: neratinib for the extended adjuvant treatment of early-stage HER2-positive breast cancer. Clin Cancer Res. 2018 Aug 1;24(15):3486-91. doi: 10.1158/1078-0432.CCR-17-3628.
29. Sohn SH, Sul HJ, Kim B, Kim HS, Kim BJ, Lim H. RNF43 and PWWP2B inhibit cancer cell proliferation and are predictive or prognostic biomarker for FDA-approved drugs in patients with advanced gastric cancer. J Cancer. 2021 Jun 1;12(15):4616-25. doi: 10.7150/jca.56014, PMID 34149925.
30. Wellington K, Keam SJ. Spotlight on bicalutamide 150mg in the treatment of locally advanced prostate cancer. Drugs Aging. 2007;24(2):169-71. doi: 10.2165/00002512-200724020-00008, PMID 17313204.
31. Meti GY, Kamble RR, Biradar DB, Margankop SBS. Synthesis of biphenyl derivatives as ACE and  $\alpha$ -amylase inhibitors. Med Chem Res. 2013 Mar;22(12):5868-77. doi: 10.1007/s00044-013-0574-8.
32. Xiao L, Wang Y, Yang J, Yuan F, Jiang C, Hou B. Determination and correlation of solubility of 4-bromomethyl-2-cyanobiphenyl in acetone+(ethanol, n-propanol, n-butanol) mixtures. The Journal of Chemical Thermodynamics. 2016;102:199-210. doi: 10.1016/j.jct.2016.06.032.
33. Hernandez Olmos V, Heering J, Planz V, Liu T, Kaps A, Rajkumar R. First structure-activity relationship study of potent BLT2 agonists as potential wound-healing promoters. J Med Chem. 2020 Oct 22;63(20):11548-72. doi: 10.1021/acs.jmedchem.0c00588. PMID 32946232.
34. Baburajeev CP, Mohan CD, Patil GS, Rangappa S, Pandey V, Sebastian A. Nano-cuprous oxide catalyzed one-pot synthesis of a carbazole-based STAT3 inhibitor: A facile approach via intramolecular C-N bond formation reactions. RSC Adv. 2016 Mar;6(43):36775-85. doi: 10.1039/C6RA01906D.
35. Gani MA, Nurhan AD, Maulana S, Siswodihardjo S, Shinta DW, Khotib J. Structure-based virtual screening of bioactive compounds from Indonesian medical plants against severe acute respiratory syndrome coronavirus-2. J Adv Pharm Technol Res. 2021 Apr-Jun;12(2):120-6. doi: 10.4103/japtr.JAPTR.88.21. PMID 34159141.
36. Kalirajan R, Sankar S, Jubie S, Gowramma B. Molecular docking studies and in-silico ADMET screening of some novel oxazine substituted 9-anilinoacridines as topoisomerase II inhibitors. Ind J Pharm Educ Res. 2017 Jan;51(1):110-5. doi: 10.5530/ijper.51.1.15.
37. Ganaie AA, Siddique HR, Sheikh IA, Parray A, Wang L, Panyam J. A novel terpenoid class for prevention and treatment of KRAS-driven cancers: comprehensive analysis using in situ, *in vitro*, and *in vivo* model systems. Mol Carcinog. 2020 Aug;59(8):886-96. doi: 10.1002/mc.23200, PMID 32291806.
38. Sun Q, Burke JP, Phan J, Burns MC, Olejniczak ET, Waterson AG. Discovery of small molecules that bind to K-Ras and inhibit



- Sos-mediated activation. *Angew Chem Int Ed Engl.* 2012 Jun 18;51(25):6140-3. doi: 10.1002/anie.201201358, PMID 22566140.
39. Lanka G, Bathula R, Dasari M, Nakkala S, Bhargavi M, Somadi G. Structure-based identification of potential novel inhibitors targeting FAM3B (PANDER) causing type 2 diabetes mellitus through virtual screening. *J Recept Signal Transduct Res.* 2019 Jun;39(3):253-63. doi: 10.1080/10799893.2019.1660897, PMID 31517548.
  40. Ibrahim RS, El-Banna AA. Network pharmacology-based analysis for unraveling potential cancer-related molecular targets of Egyptian propolis phytoconstituents accompanied with molecular docking and *in vitro* studies. *RSC Adv.* 2021 Mar 22;11(19):11610-26. doi: 10.1039/d1ra01390d, PMID 35423607.
  41. Das SK, Mahanta S, Tanti B, Tag H, Hui PK. Identification of phytocompounds from *Houttuynia cordata* Thunb. as potential inhibitors for SARS-CoV-2 replication proteins through GC-MS/IC-MS characterization, molecular docking and molecular dynamics simulation. *Mol Divers.* 2022 Feb;26(1):365-88. doi: 10.1007/s11030-021-10226-2, PMID 33961167.
  42. Ross KC, Andrews AJ, Marion CD, Yen TJ, Bhattacharjee V. Identification of the serine biosynthesis pathway as a critical component of BRAF inhibitor resistance of melanoma, pancreatic, and non-small cell lung cancer cells. *Mol Cancer Ther.* 2017 Aug;16(8):1596-609. doi: 10.1158/1535-7163.MCT-16-0798. PMID 28500236.
  43. Bhat MA, Tüzün B, Alsaif NA, Ali Khan A, Naglah AM. Synthesis, characterization, molecular modeling against EGFR target and ADME/T analysis of novel purine derivatives of sulfonamides. *Journal of Molecular Structure.* 2022;1257. doi: 10.1016/j.molstruc.2022.132600.
  44. Umar AB, Uzairu A, Shallangwa GA, Uba S. Design of potential anti-melanoma agents against SK-MEL-5 cell line using QSAR modeling and molecular docking methods. *SN Appl Sci.* 2020 Apr;2(5):1-18. doi: 10.1007/s42452-020-2620-8.
  45. Attique SA, Hassan M, Usman M, Atif RM, Mahboob S, Al-Ghanim KA. A molecular docking approach to evaluate the pharmacological properties of natural and synthetic treatment candidates for use against hypertension. *Int J Environ Res Public Health.* 2019 Mar 14;16(6):923. doi: 10.3390/ijerph16060923, PMID 30875817.
  46. Abdullahi M, Adeniji SE. In-silico molecular docking and ADME/Pharmacokinetic prediction studies of some novel carboxamide derivatives as anti-tubercular agents. *Chemistry Africa.* 2020 Jul;3(4):989-1000. doi: 10.1007/s42250-020-00162-3.
  47. Huang C, Lu HF, Chen YH, Chen JC, Chou WH, Huang HC. Curcumin, demethoxycurcumin, and bisdemethoxycurcumin induced caspase-dependent and-independent apoptosis via Smad or Akt signaling pathways in HOS cells. *BMC Complement Med Ther.* 2020;20(1):68. doi: 10.1186/s12906-020-2857-1. PMID 32126993.
  48. Peret Almeida L, Cherubino APF, Alves RJ, Dufosse L, Gloria MBA. Separation and determination of the physico-chemical characteristics of curcumin, demethoxycurcumin and bisdemethoxycurcumin. *Food Research International.* 2005 Oct-Nov;38(8-9):1039-44. doi: 10.1016/j.foodres.2005.02.021.
  49. Lu AZ, Hu TQ, Osmond DA, Patrick BO, James BR. Tetrazole ethers from lignin model phenols: synthesis, crystal structures, and photostability. *Can J Chem.* 2001 Aug;79(8):1201-6. doi: 10.1139/v01-110.
  50. Mobina L, Mehfuza M, Seema P, Ahmed A, Khan JG. Analytical method development and validation and forced degradation stability-indicating studies of Favipiravir by RP-HPLC and UV in bulk and pharmaceutical dosage form. *Nazifa Sabir Ali S J Pharm Res Int.* 2021 Nov;33(48B):254-71.
  51. Kavitha CV, Nambiar M, Ananda Kumar CS, Choudhary B, Muniyappa K, Rangappa KS. Novel derivatives of spirohydantoin induce growth inhibition followed by apoptosis in leukemia cells. *Biochem Pharmacol.* 2009 Feb 1;77(3):348-63. doi: 10.1016/j.bcp.2008.10.018, PMID 19014909.
  52. Ciapetti G, Cenni E, Pratelli L, Pizzoferrato A. *In vitro* evaluation of cell/biomaterial interaction by MTT assay. *Biomaterials.* 1993 Apr;14(5):359-64. doi: 10.1016/0142-9612(93)90055-7, PMID 8507779.
  53. Lodish H, Berk A, Zipursky SL. Proto-oncogenes and tumor-suppressor genes. *Mole cell bio.* 4<sup>th</sup> ed. New York; 2000.
  54. Donald JE, Kulp DW, DeGrado WF. Salt bridges: geometrically specific, designable interactions. *Proteins.* 2011 Mar;79(3):898-915. doi: 10.1002/prot.22927, PMID 21287621.
  55. Infield DT, Rasouli A, Galles GD, Chipot C, Tajkhorshid E, Ahern CA. Cation- $\pi$  interactions and their functional roles in membrane proteins. *J Mol Biol.* 2021 Aug 20;433(17):167035. doi: 10.1016/j.jmb.2021.167035. PMID 33957146.
  56. Xiong G, Wu Z, Yi J, Fu L, Yang Z, Hsieh C. ADMET lab 2.0: an integrated online platform for accurate and comprehensive predictions of ADMET properties. *Nucleic Acids Res.* 2021 Jul 2;49(W1):W5-W14. doi: 10.1093/nar/gkab255, PMID 33893803.
  57. Daina A, Michielin O, Zoete V. Swiss ADME: a free web tool to evaluate pharmacokinetics, drug-likeness and medicinal chemistry friendliness of small molecules. *Sci Rep.* 2017 Mar 3;7:42717. doi: 10.1038/srep42717, PMID 28256516.
  58. Isyaku Y, Uzairu A, Uba S. Computational studies of a series of 2-substituted phenyl-2-oxo-, 2-hydroxyl-and 2-acyloxyethylsulfonamides as potent anti-fungal agents. *Heliyon.* 2020;6(4):e03724. doi: 10.1016/j.heliyon.2020.e03724. PMID 32322718.
  59. Bojarska J, Remko M, Breza M, Madura ID, Kaczmarek K, Zabrocki J. A supramolecular approach to structure-based design with a focus on synthons hierarchy in ornithine-derived ligands: review, synthesis, experimental and in silico studies. *Molecules.* 2020 Mar 3;25(5):1135. doi: 10.3390/molecules25051135, PMID 32138329.
  60. Malani MH, Dholakiya BZ, Ibrahim AS, Badria FA. Synthesis and selective cytotoxicity of novel biphenyl-based tetrazole derivatives. *Med Chem Res.* 2014 May;23(10):4427-35. doi: 10.1007/s00044-014-1010-4.
  61. Karabacak M, Yilan E. Molecular structure, spectroscopic (FT-IR, FT-Raman, <sup>13</sup>C and <sup>1</sup>H NMR, UV), polarizability and first-order hyperpolarizability, HOMO and LUMO analysis of 4'-methylbiphenyl-2-carbonitrile. *Spectrochim Acta A Mol Biomol Spectrosc.* 2012 Feb 15;87:273-85. doi: 10.1016/j.saa.2011.11.051, PMID 22185952.
  62. Alici O, karatas I. Novel oximes including 4'-(n-aminoalkoxy) biphenyl-4-carbonitrile: synthesis and characterization. *J Selc Uni Nat Appl Sci.* 2014 Oct;3(3):81-91.
  63. Lestari ML, Indrayanto G. Curcumin. *Profiles Drug Subst Excip Relat Methodol.* 2014;39:113-204. doi: 10.1016/B978-0-12-800173-8.00003-9.
  64. Ciapetti G, Cenni E, Pratelli L, Pizzoferrato A. *In vitro* evaluation of cell/biomaterial interaction by MTT assay. *Biomaterials.* 1993 Apr;14(5):359-64. doi: 10.1016/0142-9612(93)90055-7, PMID 8507779.
  65. Bahuguna A, Khan I, Bajpai VK, Kang SC. MTT assay to evaluate the cytotoxic potential of a drug. *Bangladesh J Pharmacol.* 2017 Apr;12(2):115-8. doi: 10.3329/bjp.v12i2.30892.